Computer Simulation of Light Aircraft Crash

R. J. Melosh*
MARC Analysis Research Corporation, Palo Alto, Calif.
and
M. P. Kamat†
Virginia Polytechnic Institute and State University, Blacksburg, Va.

A computer prediction of postimpact response of a general aviation aircraft is reported. The analysis and response are described from the time of first runway contact based on a skeletal model that emulates material yielding and large geometry changes. The simulation models the system as a three-dimensional stiffness-equivalent truss. The material is described as an elastic-plastic-strain-hardened aluminum. Gap elements reflect the changing runway contact as the structure translates, rotates, bends, and ovalates. Recoverable and dissipated energies are determined for each time interval of the response history. The simulation results show that the response can be divided into three phases. The first phase follows initial contact. Relatively little of the kinetic energy is absorbed in structural deformation as the translational motion of the airplane is transformed into a combination of rotation and translation. The second phase, the rebound phase, follows immediately. In this phase, the body slams into the runway, inducing large decelerations and structural distortion. In the third phase, the relaxing phase, the airplane assumes a slowly diminishing angle of attack as gravity forces supercede inertial. These computer responses reflect behavior observed in films of the corresponding physical experiments. Sensitivity studies illustrate that higher fidelity of simulation requires better representation of inertial effects.

I. Introduction

COMPUTER simulation of aircraft crash, besides offering the prospect of improving crashworthiness, is an exciting challenge to the applied mechanicist. It involves the usual difficulties of multi-degree-of-freedom analysis of a complex structural geometry. These are compounded by nonlinear material behavior and significant changes to geometry with time. Since the application of numerical analysis methods to this task is relatively new, lack of knowledge on how to define an adequate idealized model is a major impediment to accuracy.

This paper describes results of such a simulation. The next section briefly defines the physical system of interest. The third section reviews the analysis assumptions. The fourth section presents computer predictions of behavior. The fifth section questions analysis fidelity by examining the effects of changing the numerical model. The last section is a collection of conclusions. This study was motivated by work performed by the authors in association with the NASA Langley project on general aviation safety.[1] Although the initial purpose of the study was to validate features of a computer code, the increased understanding of the crash justified formalizing the study as a report.

II. Physical System

An eight-passenger general aviation aircraft was destroyed in a controlled crash in the spring of 1974 by a NASA Langley laboratory team headed by Vic Vaughan. The goal of this study is to simulate that experiment. Figure 1 illustrates the test setup.[2] The pull-back cable is used to draw the airplane up to its release position in the 240-ft-high gantry structure. Upon release, the airplane rotates and translates as a pendulum mass. The swing cables, attached at each side of the airplane at the center of gravity, inhibit yaw and roll oscillations during the pendulum motion. Explosive charges separate the supporting cables from the aircraft 0.1 sec before impact with the flat concrete runway. The airplane contacts and moves down the runway in free flight. An arresting device prevents excessive excursions beyond the end of the runway. Figure 2 is a scale drawing of the complete airplane. The vehicle is 32 ft long, has a wing span of 41 ft, and a maximum body height of 62 in. With a four-man crew, the system weighs 6172 lb.

Figure 3 represents the semimonocoque construction of rolled aluminum (2024-T3) components. This figure presents a portion of the body forward of the firewall. The envelope of the airplane is maintained by a skin of constant-thickness sheets. The skin thickness increases near the middle of the passenger compartment, reflecting its structural function. The skin is supported by longitudinal stiffeners, spaced about 4 in. apart, and braced by bulkheads spaced an average of every 3 ft along the body centerline. This stiffened envelope is tied to a heavy aluminum floor structure over most of the body. This transits into the built-up beam, which serves as the nose wheel well in the structure of Fig. 3.

Each stressed skin wing has a main spar and a set of normal ribs. The main spar passes into the body floor structure. Forward and aft light spars transfer wing torsional loads to the body frame. Table 1 defines the longitudinal weight distribution of the Drop 3 airplane. The center of gravity falls 99.5 in. aft of the impact station. Almost half of the weight is represented by mocked fuel and dead weight of the wing engines.

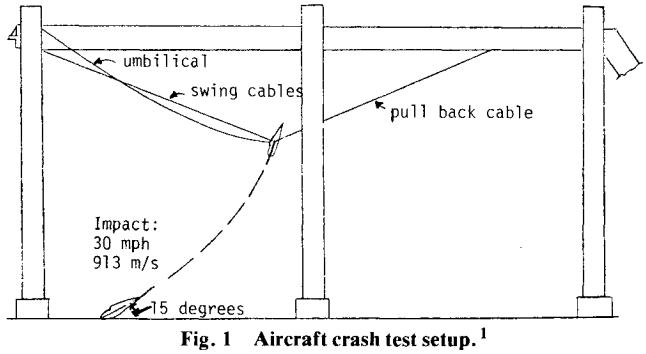

Fig. 1 Aircraft crash test setup.[1]

Received Aug. 5, 1976; revision received June 15, 1977.
Index categories: Structural Dynamics; Structural Design.
*Manager. Member AIAA.
†Associate Professor. Member AIAA.

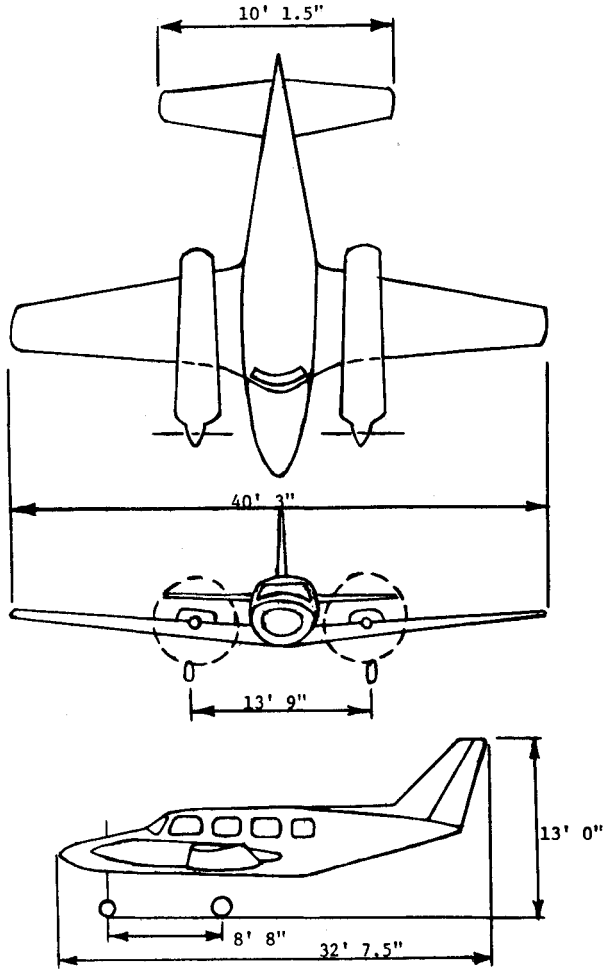

Fig. 2 Aircraft general layout.

Drop 3 involved release of the airplane 136 ft above the runway surface. Impact occurred at an angle of attack of 16° and a speed of 60 mph (87.56 fps). Measurements of the friction coefficient between the aluminum frame and the runway yielded a value of 0.56 based on a drag test of a similar configuration. After contact, the airplane pitches about the contact region until the body contacts the runway. It then rebounds, rotating to an angle of attack less than 16°.

Table 1 Test vehicle weight distribution

Station, in.[a]	Item	Weight, lb[b]
25.3	Nose	41
51.6	Engines	1474
70.5	Instrumentation	34
99.5	Miscellaneous test equipment	200
101.0	Crewman and seat	391
103.9	Wing leading-edge fuel tanks	967
123.2	Wing trailing-edge fuel tanks	700
126.5	Main landing gear	137
127.1	Fuselage and wing structure	1236
135.5	Wing aelerons	20
136.5	Passenger and seat	391
151.5	Wing flap	39
172.5	Passenger and seat	391
316.5	Fin	218
321.9	Tail, rudder	304
	Total	6172

[a] Measured from touchdown point aft along body centerline.
[b] Complete airplane.

This attitude is maintained until drag forces introduced at the end of the runway cause the airplane to settle to the ground.

III. Simulation Assumptions

The airplane structure is modeled to match the stiffness distribution for linear behavior. Gap and friction elements represent the changing contact between the airframe and the runway. Integration of the equations of motion is performed using an accuracy-controlled implicit method. Figure 4 is a plot of the finite-element model of the airplane. The model represents half of the airplane; the configuration is implied to be symmetric across the centerplane.

The model involves 92 line elements reflecting the three-dimensional geometry of the body envelope. The half cross section of the body is articulated as a triangular section. Most of the elements lie forward of the passenger compartment to provide a more detailed representation of the structure in the region of runway contact.

The element cross-sectional areas are chosen to represent the undeformed volume of skin, stiffeners, and bulkheads. The longitudinal elements are assigned areas equal to the total area of skin and longitudinal stiffners. Similarly, areas of vertical elements match the area of material in skin and bulkheads. Areas of diagonal elements are selected to match the shear stiffners of the skin in each bay, neglecting skin

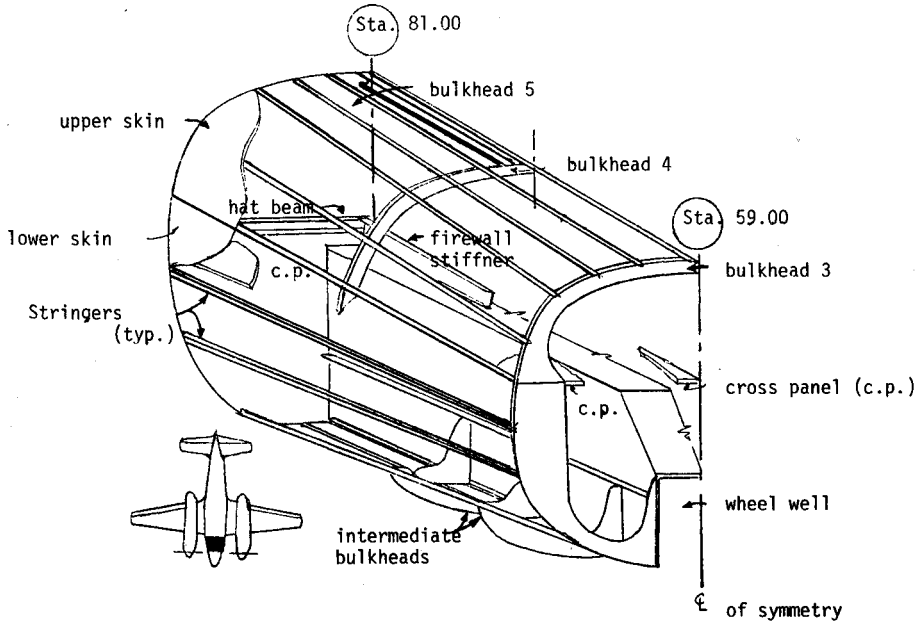

Fig. 3 Representative fuselage structure.

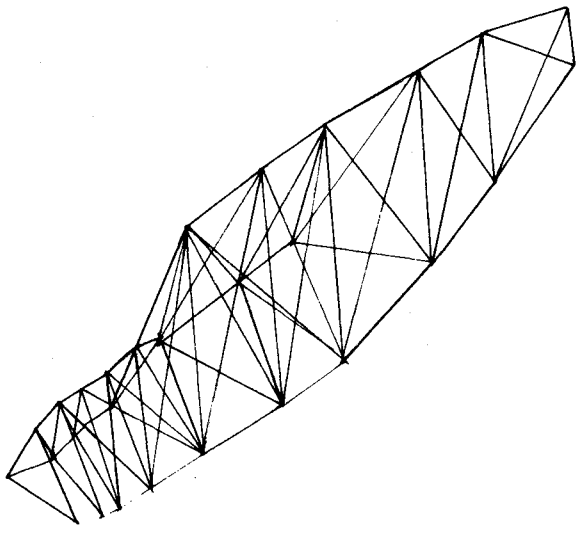

Fig. 4 Airplane crash finite-element model.

curvature. The nose closure section, the wings, and the tail structure are omitted. The nose section is of fiberglass. It shatters upon impact. Since the experiment results in no permanent deformations of the wings, they are assumed rigid. The tail structure was not on the test vehicle.

The masses given in Table 1 were redistributed to finite-element joints, preserving the total mass and center-of-gravity position. The fuel, engine, and passengers were represented as rigid point masses. The fuel tanks of the prototype are thus assumed to be full, the engines stopped, and the passengers immobile.

Table 2 cites the breakpoints of the equivalent stress-strain curve used in the analysis. The first plus and minus nonzero stresses define the tensile and compression yield stresses. Compression stresses are reduced to reflect tension field effects in the forward position of the body. Kinematic hardening is assumed. Damping associated with internal material friction is neglected as small in comparison with plastic work. The analysis was initiated with an appropriate joint in contact with the rigid runway model. All other joints were required to have a velocity of 87.56 fps along the airplane centerline. Coordinates were assigned so that the centerline of the vehicle model would make an angle of 16° with the runway.

Gap elements were used at nodes, along the contact contour. These provide no resistance to motion until the vertical distance between the runway and the node is closed. Then, they introduce friction forces 0.56 times the normal forces and prevent penetration of the runway plane. These gaps do not admit reopening until a force is exerted by the rest of the airplane to draw the joint off the runway. Thereby, they simulate a plastic collision between the airplane and runway.

The analysis was implemented using the ACTION code.[3,4] This code discretizes time, assuming that response in each degree of freedom varies as a cubic polynomial in time. It satisfies equilibrium at the end of the time step, thereby providing an implicit integration method. It obtains the stepwise solution of the equations of motion by direct minimization of the total potential energy. Thus, it finds the geometry, velocity, and accelerations at the end of each time step which define a dynamic equilibrium configuration.

Five digits of accuracy were required in the energy minimization using ACTION. The code interprets this as a requirement to reduce the energy associated with unbalanced forces to less than 0.1×10^{-4} of the energy change. Time steps are selected automatically so that the error at midstep times, based on interpolated configuration data, is less than 0.1×10^{-3} times the energy change.

Table 2 Stress-strain curve breakpoints[a]

Tension		Compression	
Stress, psi	Strain	Stress, psi	Strain
0.	0.	0.	0.
52,000[b]	0.005	−36,000[b]	−0.0034
54,000	0.0096	−50,000	−0.0098
58,000	0.0188	−58,000	−0.0188
64,000	0.0230	−64,000	−0.0230

[a] Of folded equivalent stress, equivalent strain curve. Curve shifts in compliance with kinematic hardening law.
[b] Yield stress.

IV. Postimpact Behavior

Computer results show that postimpact response involves three different phases: initial contact, rebound, and relaxation. From the viewpoint of crashworthiness engineering, the rebound phase is the most important. Figure 5 represents the three response phases.

The initial contact phase extends from the time the airplane first touches the runway until the airplane centerline is nearly parallel to the runway – about 130 msec for the 60-mph, 16° crash. During this period, the translational motion is converted to a rotational and horizontal translation. The plastic work in the structure occurs only in the neighborhood of the runway/airplane contact.

The rebound phase extends from the end of the initial contact phase until the airplane angle of attack with the runway stops increasing, i.e., until about 260 msec after touchdown. This phase evokes relatively large plastic energy dissipation as yield stresses are exceeded in the body floor and adjacent structure.

The relaxation phase extends from the end of the rebound phase until the airplane is at rest, i.e., from 260 to 480 msec after touchdown. Motion in this phase is almost entirely horizontal translation. The angle of attack with the horizontal gradually moves toward zero as airplane/runway friction persistently absorbs the bulk of the remaining kinetic energy of impact.

The relaxation phase extends from the end of the rebound phase until the airplane is at rest, i.e., from 260 to 480 msec after touchdown. Motion in this phase is almost entirely horizontal translation. The angle of attack with the horizontal gradually moves toward zero as airplane/runway friction persistently absorbs the bulk of the remaining kinetic energy of impact.

Figure 6 shows plastic and friction energy dissipation for the first two phases of response. Friction is the maximum energy-reduction device. Since the relaxation phase extends over the longest period of time, this phase involves the maximum frictional work. Plastic work is relatively small, amounting to a total of less than 3% of the touchdown kinetic energy.

Figures 7 and 8 show the spatial allocation of energy stored as elastic work in the initial contact and rebound phases. These graphs suggest that much of the airplane involves little elastic deformation during impact. Since regions of maximum stored energy are regions where plastic work usually occurs, these plots also reflect the diffusion of plastic work away from impact contact regions as a function of time.

Figures 9 and 10 show the history of decelerations at the pilot station after contact. These data exhibit both high-frequency content and maximum amplitudes in the rebound phase. They show both lower frequencies and peaks in the initial contact phase. The direction of the deceleration vector, shown in the circles of Fig. 10, indicates a full 360° rotation with time. This suggests a need for enlarging the scope of criteria for human tolerance for the aircraft crash conditioning.

It is noted that either the initial contact or the rebound phase deceleration history would be fatal based on Gadd's severity index.[5] This suggests that safety improvements may be divisible into distinct redesign for each of the first two (the

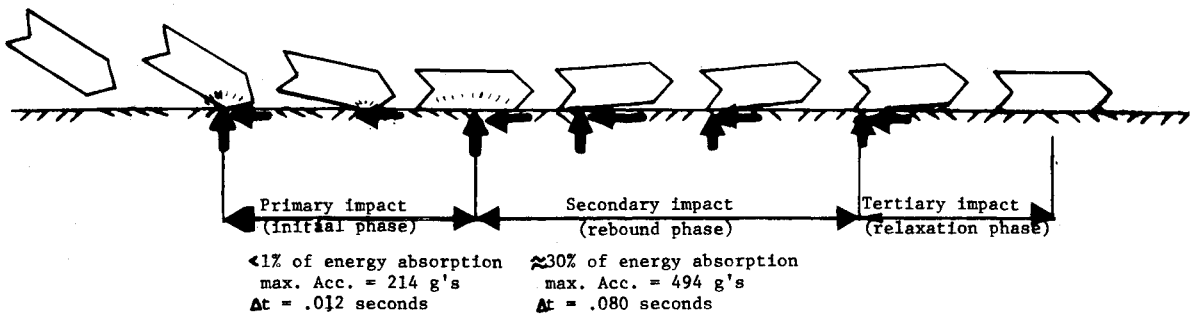

Fig. 5 Three phases of aircraft postimpact behavior.

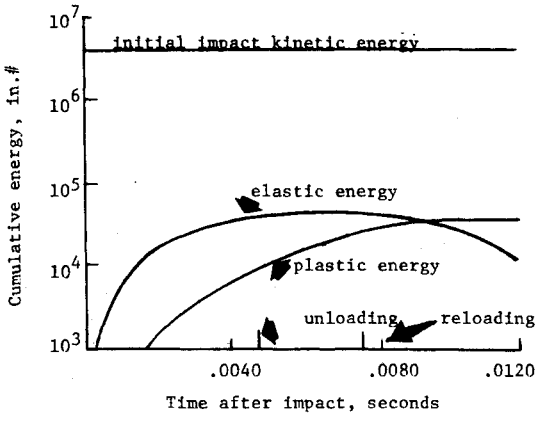

a) Time allocation of impact energy

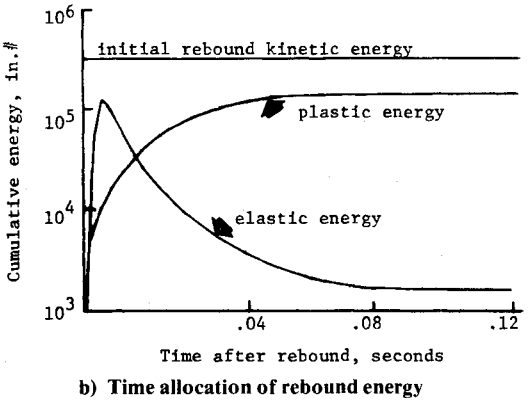

b) Time allocation of rebound energy

Fig. 6 Elastic and plastic energy time histories.

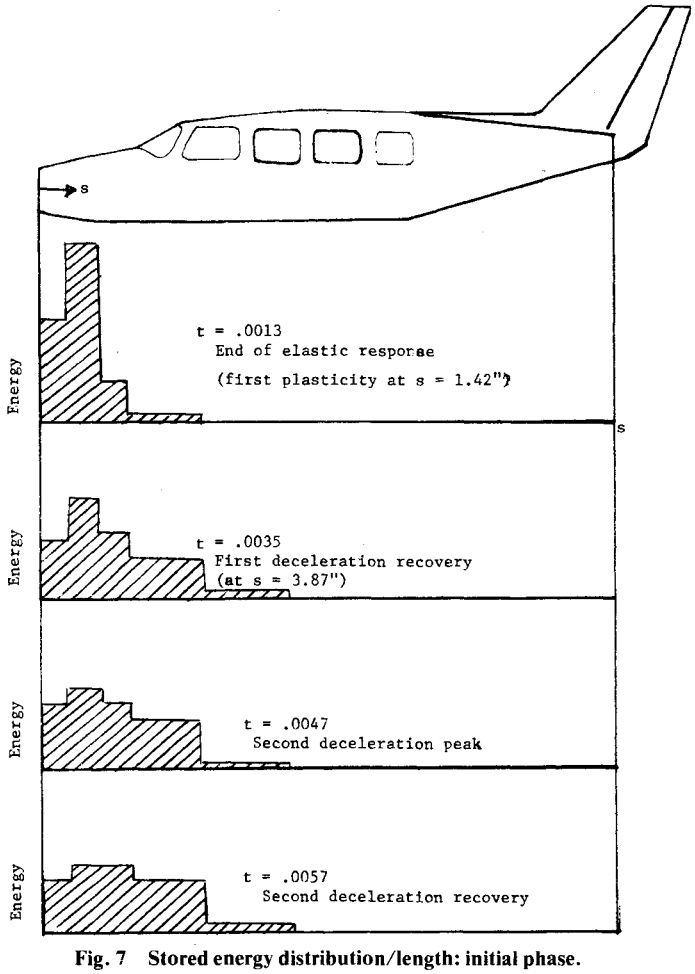

Fig. 7 Stored energy distribution/length: initial phase.

killing) phases. The fact that the rebound phase is much more hazardous than the other phases may provide the basis for extending test data or reducing the number of tests to cover the range of impact angles.

V. Analysis Accuracy

Questions on the adequacy of the finite-element and constitutive models can be answered by model sensitivity studies.[7] This section describes studies performed with the MARC code[6] to evaluate the quality of results reported in Sec. 4. Finite-element model adequacy can be inferred from studies with different numbers of elements and equations of motion. Figure 11 shows results of such studies for the initial contact phase. The continuous curve of Fig. 11 displays the time history of response for the nominal model. This model consists of 92 elements and 33 equations of motion. The reduced-elements curve, shown dashed, is associated with a finite-element model with only 73 elements and 33 equations of motion. The reduced-equations model retains all elements, but the number of equations of motion is reduced to 21 by using fewer mass points to model the total mass and mass moment.

The figure shows that general characteristics of response are preserved in the reduced-elements model. The peak acceleration occurs at the same time as that of the nominal model and is less than 5% higher. The decay of deceleration at the end of the phase initiates about the same time and decreases at the same rate in both models. Thus, the nominal model may provide an adequate representation of the geometry of the airplane.

The reduced-mass model, on the other hand, projects response significantly different from the nominal model. The maximum deceleration of the reduced-mass model is 30% lower, occurs much sooner, and reflects much lower frequency content than the nominal. Thus more equations of motion probably are needed for the nominal model to produce deceleration traces of adequate fidelity to compare with experimental data. The present nominal model is regarded as adequate only for predicting gross response

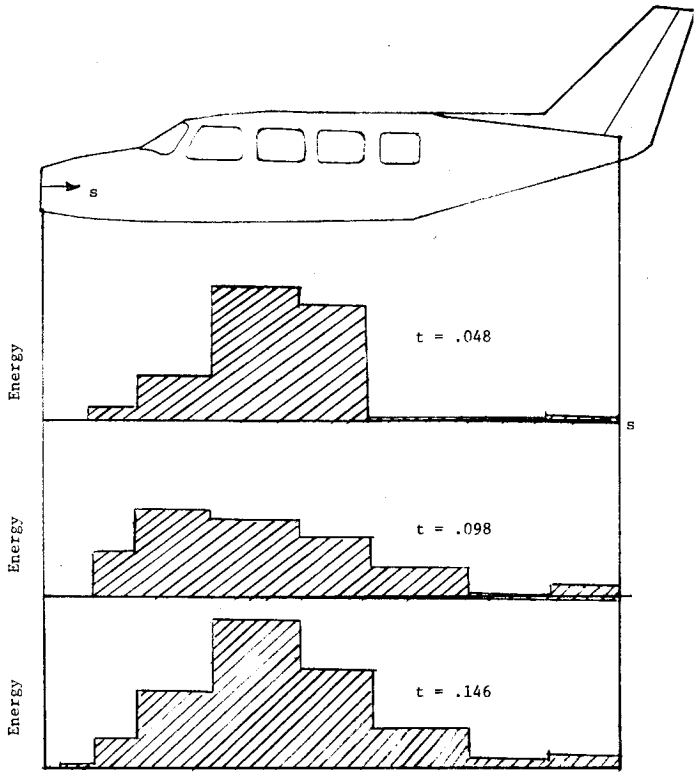

Fig. 8 Stored energy distribution/length: rebound phase.

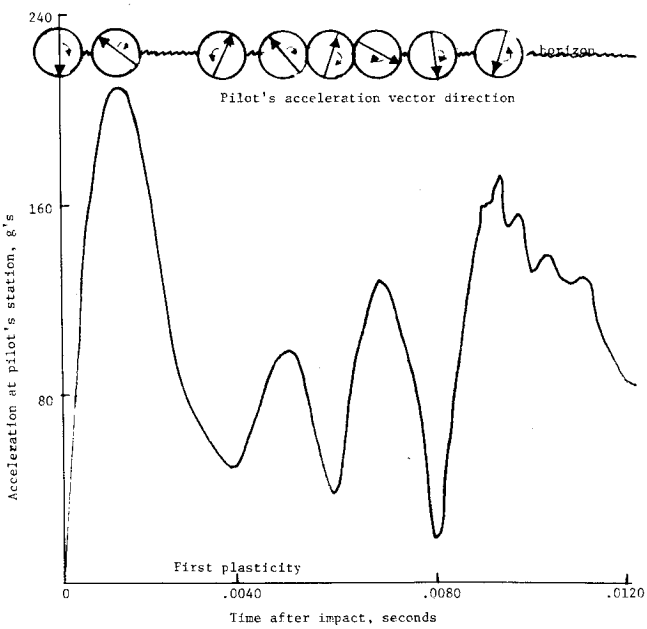

Fig. 9 Pilot's acceleration after initial impact.

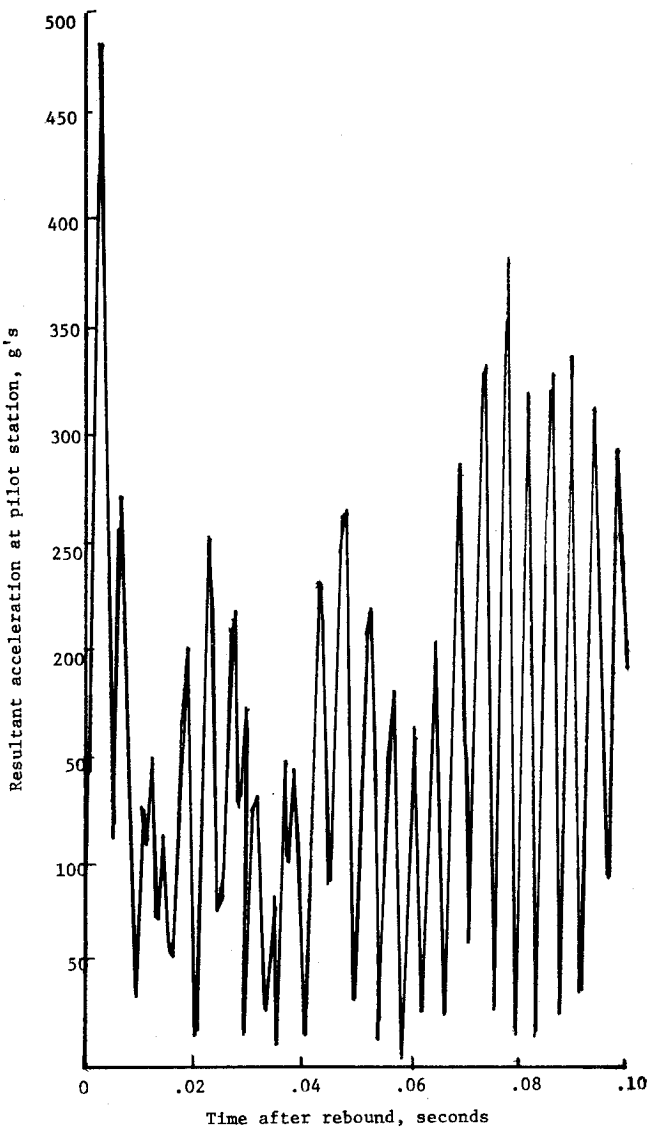

Fig. 10 Pilot's acceleration after rebound impact.

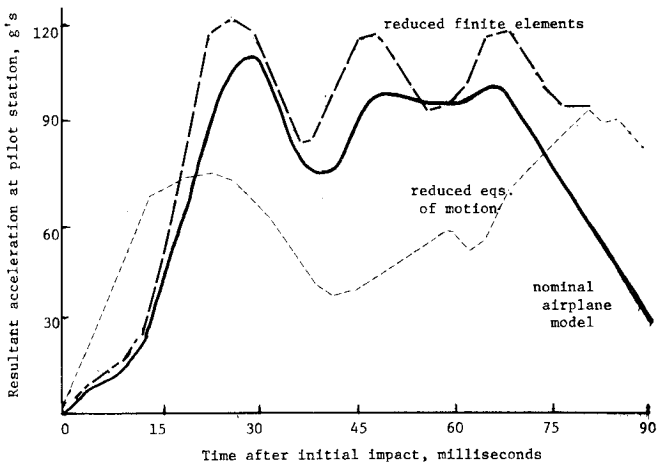

Fig. 11 Effect of modeling parameters on response predictions.

characteristics, such as the average body motion and the allocation of dissipation and stored energy.

To assay the adequacy of the representation of material characteristics, response predictions were developed with yield and breakpoint stresses reduced by 25%. Figure 12 facilitates comparing these results with those of the nominal model. The small differences in response of these two curves suggest the insensitivity of response to constitutive models. Thus, strain-rate effects, normally small in aluminum, probably can be disregarded. Simplified constitutive models, involving rigid-plastic or elastic-perfectly plastic, may provide adequate response predictions at reduced cost.

VI. Conclusions

The simulation of a controlled airplane crash furnishes the following conclusions:

1) Postimpact response involves three phases. Of these, the rebound phase is the most severe from the viewpoint of

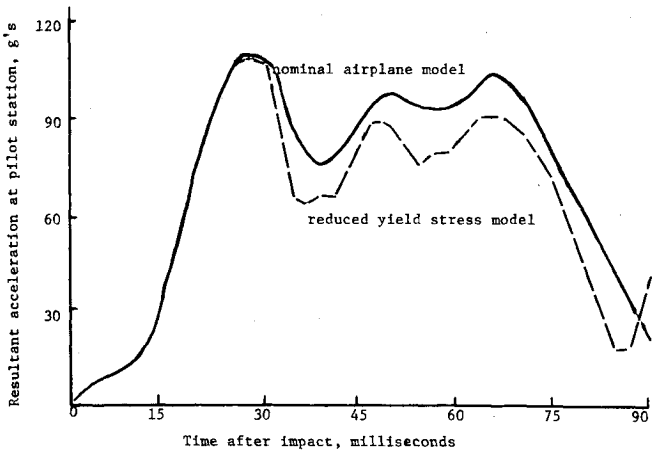

Fig. 12 Effect of yield stress on initial impact response.

passenger trauma, peak acceleration, and structural plastic work dissipation.

2) The major energy-dissipation device is airplane/runway friction. Energy consumed by plastic work is less than 3% of the touchdown kinetic energy.

3) Sensitivity studies suggest that the skeletal model is satisfactory for predicting the gross characteristics of response: mean motion vs time and energy allocation. They indicate that a material model simpler than an elastic-plastic model with kinematic hardening may provide adequate response accuracy.

The study suggests reducing and interpreting test data based on the configuration at the start of the rebound phase.

References

[1] Hayduk, R. J. and Thomas, R. G., "Simulation of Aircraft Crash and Its Validation," *AIAA 11th Annual Meeting and Technical Display*, Washington, D. C., Feb. 1975.

[2] Vaughan, V. L. and Alfaro-Bou, E., "NASA Langley Impact Dynamics Facility," *1974 SAE Business Aircraft Meeting and Engineering Display*, Wichita, Kansas, April 1974.

[3] Killian, D. E., Melosh, R. J., Swift, G. W., and Kamat, M. P., "User's Guide to the ACTION Code," Virginia Polytechnic Inst. and State Univ., Blacksburg, Va., 1974.

[4] Kamat, M. P., Killian, D. E., Melosh, R. J., and Swift, G. W., "Theoretical Basis for the ACTION Computer Code," Virginia Polytechnic Inst. and State Univ., Blacksburg, Va., 1975.

[5] Gadd, C. W., "Use of a Weighted Impulse Criterion for Estimating Head Injury," Society of Automotive Engineers, SAE Paper 660793, New York, 1966.

[6] "MARC-CDC Nonlinear Finite Element Analysis Program," Vols. I and II, Control Data Corp., Rev. G, 1974.

[7] Melosh, R. J., "Crashworthiness Engineering of Automobiles and Aircraft: Progress and Promise," AIAA Paper 75-270, Washington, D. C., Feb. 1975.